Variability in Color Discrimination Data Explained by a Generic Model with Nonlinear and Adaptive Processing

David Alleysson,* Jeanny Hérault

Laboratoire des Images et des Signaux LIS-INPG/UJF, 46 av. Felix Viallet 38031 Grenoble Cedex, France

Received 27 August 1999; accepted 27 October 1999

Abstract: A generic model of color discrimination is presented. It involves adaptive nonlinearities at photoreceptor level and in color-opponent pathways. This model, with few parameters, can reproduce the various aspects of the observed data from six individual observers, as reported in studies by MacAdam, Wyszecki and Fielder, and Brown and MacAdam. It is base on two main hypotheses: (1) all the observers have the same kind of nonlinear adaptive functions; (2) each observer has his or her own coding of color oppositions. Therefore, for each observer, the mean model parameters are adjusted to fit all the data in the particular available experimental conditions. The model is unique, one set of its parameters depends only on the adaptation state, the other set depends only on observer's specific color coding. We conclude that the observed variability in color discrimination data stem only: (1) from both difference in adaptation states, due to experimental conditions; (2) from inter-observers color coding differences. © 2000 John Wiley & Sons, Inc. Col Res Appl, 26, S225–S229, 2001

Key words: color discrimination; non linearity; biological model; color adaptation

INTRODUCTION

Discriminating among colors is a very important function of the human visual system, and many experimental studies have addressed the human ability to detect color differences. Color-matching methods have been used to help understanding color discrimination through the analysis of an observer's just noticeable differences (JND) between two lights. Through such an analysis, MacAdam[1] showed that color discrimination thresholds can be modeled by ellipses in the chromaticity plane that are centered on the chromaticities of the lights to be matched. The size and shape of a discrimination ellipse depends on the choice of the reference light. Wyszecki and Fielder[2] showed that discrimination ellipses vary from individual to individual and from one measurement to the next one for a given individual.

We present here a model of color discrimination that can account for the ellipses found for different observers and for different experimental conditions, while explaining the variability of experimental data. The model allows us to compare results from different studies, and its parameters may be interpreted in terms of biological functions.

DESCRIPTION OF EXPERIMENTAL DATA

We have chosen to work with color-matching data from six observers obtained under different experimental conditions. The data from the first observer, PGN,[1] provide color discrimination for a set of reference lights presented on a constant background level. Matching lights varied in chromaticity but not in luminance. With two further observers, WRJB and DLM,[3] data were collected using matching lights that varied both in chromaticity and luminance. The three final observers, GF, AR, and GW,[2] provide data on adapting backgrounds, using matching lights that varied both in chromaticity and luminance.

First, we convert the ellipsoids fitted to data in *xyl* space (where luminance *l* is measured in units of footlamberts) into ellipsoids expressed in the space of the cone photoreceptors' excitations. The excitations of long-, medium-, and short-wavelength sensitive photoreceptors define the *LMS* space. To convert ellipsoids in *xyl* space to *LMS* space, we first transform the equation that describes an ellipsoid in *xyl* space into one that describes the same ellipsoid in the *XYZ* space of CIE 1931 standard observer tristimulus values.

---

* Correspondence to: David Alleysson, Laboratoire des Images et des Signaux LIS-INPG/UJF, 46 av. Felix Viallet 38031 Grenoble Cedex, France (e-mail: alleysso@lis-viallet.inpg.fr)

Then we convert them from *XYZ* to *LMS* using the matrix presented by Smith and Pokorny.[4]

An ellipsoid is defined by a second-order equation of the form

$$\mathbf{V}^T\mathbf{B}\mathbf{V} = 1, \tag{1}$$

where **B** is a symmetric matrix that describes the ellipsoid parameters, and **V** is a vector that describes a difference in chromaticity and in luminance given by

$$\mathbf{V} = [dx\ dy\ dl]^T, \tag{2}$$

which is the difference between the coordinates $[x\, y\, \ell]$ of an arbitrary light and the coordinates $[x_0\, y_0\, \ell_0]$ of a reference light upon which the ellipsoid is centered:

$$dx = x - x_0,\ dy = y - y_0, \text{ and } dl = l - l_0. \tag{3}$$

The relationship between *xyl* space and the CIE *XYZ* space is given by[5]

$$X = xY/y,$$

$$Y = 10^{5l}, \text{ and}$$

$$Z = (1 - x - y)Y/y. \tag{4}$$

The linear transformation from *XYZ* tristimulus values to *LMS* cone excitations is described by a matrix $\mathbf{A}$[4]:

$$[L\ M\ S]^T = \mathbf{A} \cdot [X\ Y\ Z]^T. \tag{5}$$

The symmetric matrix **G**, which describes an ellipsoid in *LMS* space, is given in terms of the corresponding matrix **B** in *xyl* space as follows:

$$\mathbf{G} = \mathbf{J}^T\mathbf{B}\mathbf{J}, \tag{6}$$

in which **J** is the Jacobian of the transformation between *xyl* and *LMS* spaces.

Figure 1 shows color discrimination ellipsoids for observers GF and WRJB in LMS space. The ellipsoids are displayed as cross-sections in planes of the *LMS* space. For observer GF, we can see in the *LM*-plane projection (left panel) that the narrowest ellipses in the *LM* plane lie centrally, as pointed out earlier by LeGrand[6] and Nagy.[7] This generates a V-shaped function of chromatic sensitivity along a path going through the ellipses from the upper-left to lower-right of the diagram. This feature of GF's data is not apparent in the data of WRJB, presumably because discriminability was measured in this case at a different luminosity level.

THREE LAYER MODEL

Our model of color processing has three layers (see Fig. 2). The first layer simulates the photoreceptor with adaptive nonlinearities, acting independently within each class of photoreceptor, and being governed by the state of adaptation to the background (*L0 M0 S0*). Photoreceptors are known to be nonlinear and adaptive, in order to operate over a wide range of incident light levels. We have chosen a Naka–Rushton law to describe the photoreceptor response *R*:

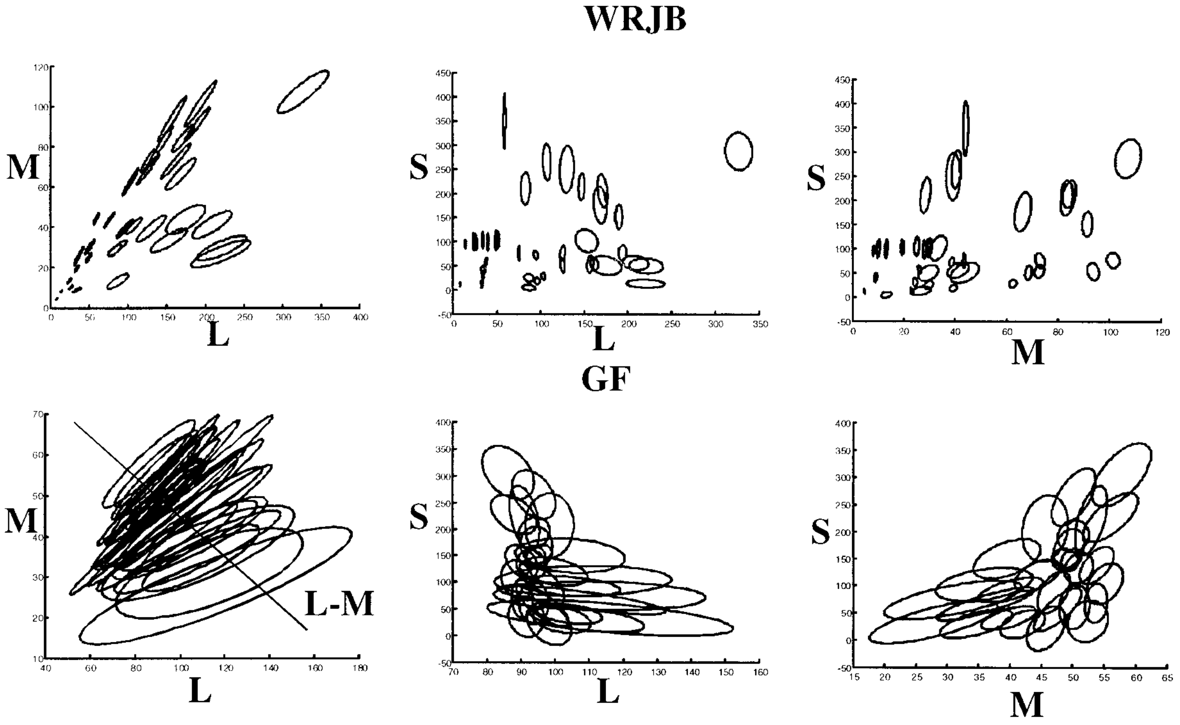

FIG. 1. Ellipsoids in *LMS* space for observers WRJB and GF enlarged 10 times. The bottom left image shows the «V» shape function (see text). The narrowest ellipses are in the center of diagram in *LM* cut (left image).

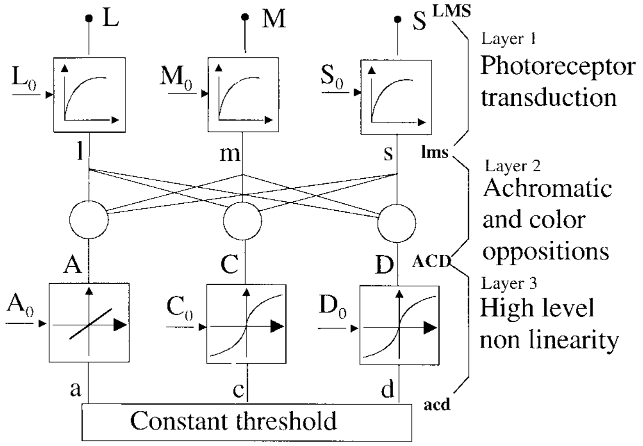

FIG. 2. The three layers model input are ellipsoids in *LMS* space. The first layer transforms these ellipsoids into ellipsoids in *lms* space through the nonlinear and adaptive transduction of the photoreceptors. The second layer transforms the *lms* ellipsoids into *ACD* ellipsoids, through a linear combination of channels into one achromatic (*A*) and two chromatic (*C, D*) channels. The third layer transforms the ellipsoids in *ACD* into ellipsoids in *acd* space through a second nonlinearity.

$$R = X/(X + X0), \tag{7}$$

in which X is the photoreceptor excitation level and $X0$ corresponds to the background level to which the photoreceptor is adapted. As shown in Fig. 3, the behavior of the nonlinearity within a particular range of excitation level depends on the choice of the background level. As shown in Fig. 2, the outputs of the first layer are the signals *l*, *m*, and *s* of the three photoreceptor classes.

The second layer of the model is linear and provides color-opponent coding. It transforms *l*, *m*, and *s* signals into an achromatic signal *A* and two color-opponent signals *C* and *D*. The coefficients that describe the color-opponent transformation of an observer should be adjusted, in order to optimally match the data.

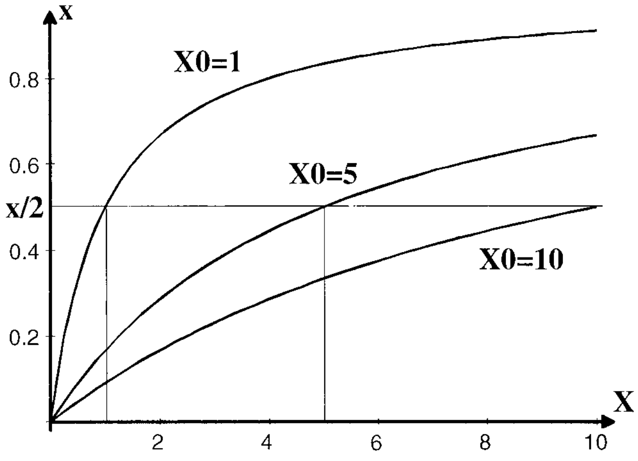

FIG. 3. The photoreceptor nonlinear transduction function has different curvatures following the adaptation state *X0*. We make the hypothesis that a constant adaptation state applied independently on the three kinds of photoreceptors (constants *L0, M0, S0*), allows us to transform ellipsoids in *LMS* space into spheres in *acd* space.

The third layer of the model (see Fig. 2) is also nonlinear and simulates a high-level adaptive compression. The function of this layer depends on the independently set adaptation levels (*A0*, *C0*, *D0*) of the achromatic and color-opponent channels. This layer's nonlinearity is described by

$$R = \arctan(X/X0), \tag{8}$$

which is similar to the Naka–Rushton law of Eq. 7, but can take into account both positive and negative input signals *A*, *C*, and *D*. It is equivalent to two Naka–Rushton laws, one for positive and one for negative variation of color opposition.

The third layer output signals *a*, *c*, and *d*. In our model, the *acd* space corresponds to the "perceptual space" in which color discrimination judgments are to be made; hence, the transformation of ellipses from *LMS* space into *acd* space.

We adjust the model parameters so that the observer's color discrimination ellipsoids are as spherical as possible in *acd* space. The model parameters found in such a way, for each observer, describe the state of adaptation and color opposition coding for this observer.

MODEL APPLICATION TO DATA

By applying the Naka–Rushton nonlinearity (Eq. 7) to photoreceptor signals only, it would be possible to transform ellipsoids in *LMS* cone excitation space into a sphere in the (adapted) *lms* space, only if the ellipsoid's axes were aligned along the *L*, *M*, and *S* axes (see Fig. 4). Yet color discrimination data show that the ellipsoids are oriented more along achromatic and color-opponent axes. We thus need color-opponent processing to transform basis axes *L*, *M*, and *S* into *A*, *C*, and *D*. But these signals *A*, *C*, and *D* are

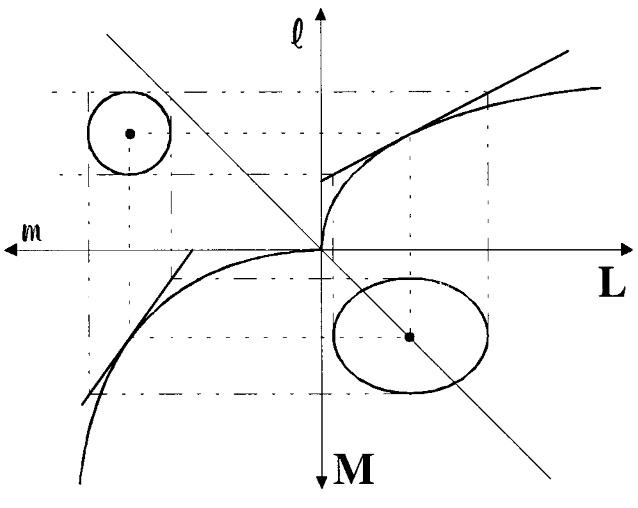

FIG. 4. A graphical example of transforming ellipses in *LMS* space into circles in *lms* space. If the axes of the ellipses are parallel to *L* and *M* axes, it is always possible to transform these ellipses into circles by the nonlinear law.

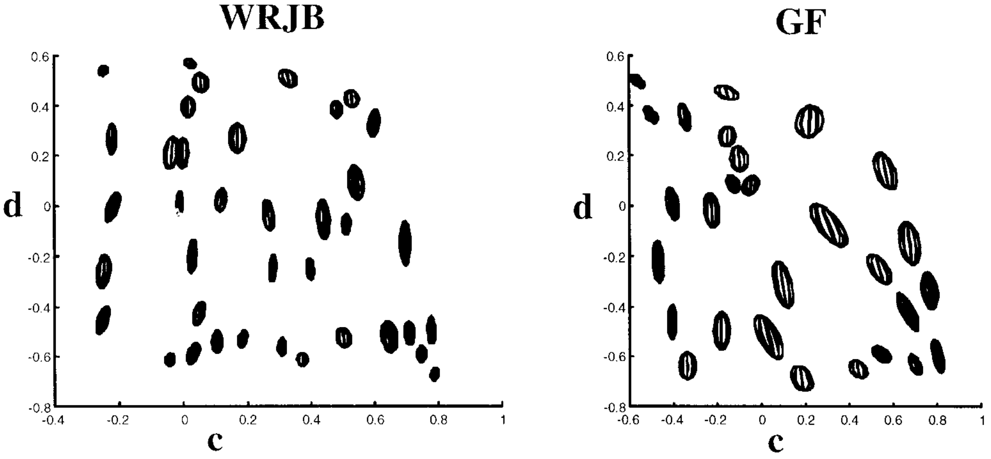

FIG. 5. Ellipsoids in *acd* space. The ellipsoids are not perfectly transformed into spheres, but the difference between any two ellipsoids is less in *acd* space than in *LMS* space. Because the ellipsoids do not have unique sizes and orientations, we may consider that this is due to measurement noise, for the main reason that the variations do not exhibit any coherence.

still not sufficient to explain the above-mentioned V-shaped function of chromatic sensitivity. For that, a compressive nonlinearity (Eq. 8) must be applied to provide *a*, *c*, and *d* signals, which can exhibit V-shaped sensitivities.

An ellipsoid in *acd* space is defined by the following equation:

$$\mathbf{Z}^T\mathbf{H}\mathbf{Z} = 1, \tag{9}$$

in which vector **Z** is given by

$$\mathbf{Z} = [da\ dc\ dd]^T = [a - a_0\ c - c_0\ d - d_0]^T, \tag{10}$$

and in which the symmetric matrix **H** is given by

$$\mathbf{H} = (\mathbf{N}^{-1})^T(\mathbf{P}^{-1})^T(\mathbf{M}^{-1})^T\mathbf{G}\quad \mathbf{N}^{-1}\mathbf{P}^{-1}\mathbf{M}^{-1}. \tag{11}$$

The terms in Eq. 11 include symmetric matrix **G**, which describes the ellipsoid in *LMS* space (Eq. 6); matrix **M**, which is a linear approximation of the first nonlinearity (Eq. 7), is determined at the center of the ellipsoids in *LMS* space; matrix **P**, which describes linear color-opponent coding, and matrix **N**, which is a linear approximation of the second nonlinearity (Eq. 8), found at the center of the ellipsoids in *ACD* space.

We use a classical gradient descent algorithm to fit the color discrimination data, with a cost function *J* as follows:

$$J = (\mathbf{H} - \mathbf{I})^T(\mathbf{H} - \mathbf{I}), \tag{12}$$

in which an *acd* space ellipsoid, represented by matrix **H**, is compared to a sphere in *acd* space, represented by the identity matrix **I**. The model adaptation parameters *L0, M0, S0, A0, C0, D0*, and color-opponent transformation parameters of matrix **P**, are computed in order to minimize the cost *J*, for each observer and each experimental condition. This results in choosing model parameters that make the color discrimination ellipsoids in *acd* space as spherical as possible.

RESULTS AND CONCLUSION

Color-discrimination ellipsoids for observers WRJB and GF are shown in the *cd* chromaticity plane of *acd* space in Fig. 5. The loci of Just Noticeable Differences in *acd* space approximate spheres much better than they do in *LMS* space. Table I shows model parameters, which depend on observers and experimental conditions.

To estimate how well the model fits the data, we replace all the ellipsoids in *acd* space by an average ellipsoid (instead of taking a mean sphere, we use the mean ellipsoid to take into account an unknown scale parameter in the *acd* space) and then, through a reverse transformation, compute the corresponding ellipsoid in *LMS* space. Figure 6 shows what the single, average ellipsoid in *acd* space looks like when transformed back to the original *LMS* space. Our model explains the orientation and size of each observer's ellipsoids when the adaptation state is kept constant. It can

TABLE I. Parameters estimated for the three layers model. We can see that the parameters are close to each other for the same experimental condition (PGN alone, WRJB and DLM, GF and AR and GW), but may vary substantially between two different experimental conditions.

Param.\Obs.	PGN	WRJB	DLM	GF	AR	GW
L0	141	78	65.2	103	96	96
M0	79	39	32.7	50	45	43
S0	1320	98	95.5	149	135	139
C0	.08	.09	.07	.04	.04	.04
D0	1.19	0.28	0.28	0.17	0.18	0.14

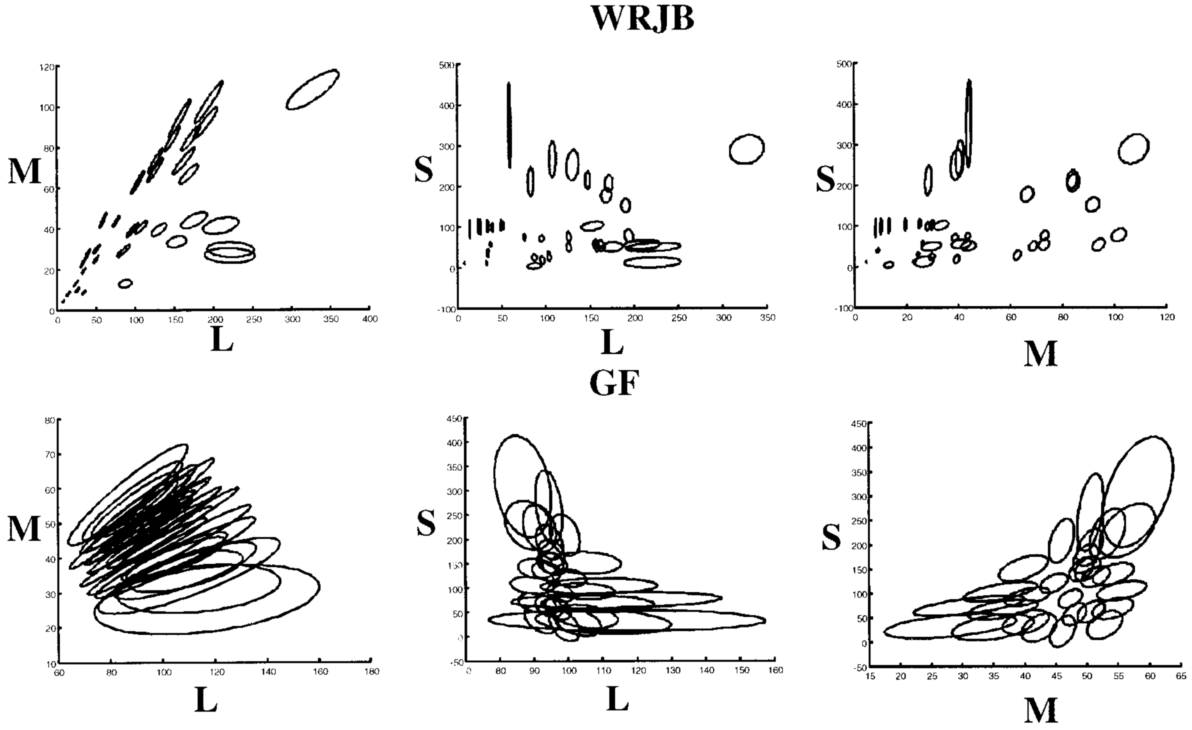

FIG. 6. Reconstruction of ellipsoids in *LMS* space from the average ellipsoid in *acd* space. (Compare with the ellipsoids of Fig. 1.) We see that the global orientations and sizes of the ellipsoids are well reproduced despite the strong differences between the observers, and that the «V» shape function is well reproduced for observer GF.

exhibit a large variety of sizes and orientations in *LMS* space (Fig. 6), which match the original data (Fig. 1) very well. Note also that the model matches the V-shaped sensitivity along the top-left to bottom-right diagonal in the *LM* plane of observer GF's data, without giving rise to a similar effect on WRJB's data.

We have attempted to explain the variability in color discrimination through a biologically motivated model, whose parameters depend on the observer's coding scheme and adaptation state. The success of this attempt, clearly shown when comparing Figs. 1 and 6, is a strong motivation for the use of biologically motivated hypotheses for the studies of color-vision processing.

ACKNOWLEDGMENTS

We thank A. Taleb for his help with the gradient descent algorithm used in this study, and for discussion of nonlinearities. We also thank the reviewers for their help in making this article more readable.

1. MacAdam DL. Visual sensitivities to color differences in daylight. J Opt Soc Am 1942;32:247–273.
2. Wyszecki G, Fielder GH. New color-matching ellipses. J Opt Soc Am 1971;61:1135–1152.
3. Brown WRJ, MacAdam DL. Visual sensitivities to combined chromaticity and luminance differences. J Opt Soc Am 1949;39:808–834.
4. Smith VC, Pokorny J. Spectral sensitivity of the foveal cone photopigments between 400 and 500 nm. Vision Res 1975;15:161–171.
5. Wyszecki G, Stiles WS. Color science: quantitative data and formulae. 2nd Ed. New York: John Wiley; 1982.
6. LeGrand Y. Les seuils differentiels de couleur dans la théorie de Young. Rev Opt 1949;28:261–278. (Translation: Knoblauch K, translator. Color difference threshold in Young's theory. Color Res Appl 1994;19:296–309.)
7. Nagy AL, Eskew RT, Boynton RM. Analysis of color-matching ellipses in a cone-excitation space. J Opt Soc Am 1987;4:756–768.